Invited Paper

Modeling Scatter in Composite Media

Eric C. Fest
Raytheon Missile Systems, 1151 E. Hermans Road Bldg 840 M/S 4, Tucson, AZ 85706
eric@raytheon.com, Phone: 520-545-7701, Fax: 520-794-0872

ABSTRACT

A theoretical model of optical scattering in materials consisting of densely packed spherical particles is developed that can be used to predict its optical properties given its physical characteristics. The inputs to this model are the waveband of interest, the complex refractive indices and particle size distribution of the materials that comprise the media (including any contaminants), the density and sizes of any contaminants in the media, and the dimensions of the media slab. The outputs of this model are the specular transmittance and emissivity vs. wavelength of the media, and it's Bidirectional Scattering Distribution Function (BSDF) vs. scatter angle vs. wavelength. The results of this model are compared to measured transmittance and BSDF data from optical ceramics comprised of densified nanopowders (nanocomposite optical ceramics).

Keywords: Scatter, Mie, Rayleigh, dense media, composite media, optical ceramics, BSDF

1. INTRODUCTION

An optical model of media that consists of densely packed spherical particles is developed in order to predict its optical performance (transmittance and BSDF) as a function of wavelength and incident polarization. The optical performance is determined in this model from the electric field scattered by the particle collection, hence the emphasis on computing scatter. This model is important in that it allows pre-selection of these materials prior to fabrication, which is often expensive, and can be used to identify the presence of contaminants in the material. This model takes as input the waveband of interest, the complex refractive indices and particle size distribution of the materials that comprise the media (including any contaminants), the density and sizes of any contaminants in the media, and the dimensions of the media slab. An example of such a material is a nanocomposite optical ceramic (NCOC), which is being investigated for use in mid-wave IR (3-5 μm) optical systems that are subjected to high mechanical and thermal stress, such as cameras used in aerospace applications. A scanning electron micrograph (SEM) of an NCOC sample is shown in Figure 1. The sample shown consists of nanoparticles of yttria (Y_2O_3) and magnesium oxide (MgO) that have been densified using a hot isostatic press (HIP) process. This process is carefully controlled to avoid percolation (melting together) of the nanoparticles and to reduce the number of pores. Maintaining the integrity of the nanoparticles increases the strength of the material and (as will be shown) reduces scattering [1].

Another advantage of NCOCs that is demonstrated in this paper is that their refractive index and dispersive properties (Abbe number) can be chosen by changing the volume fractions of their constituent materials. This is not possible with traditional glasses and IR materials whose refractive index and Abbe number are fixed. Figure 2 illustrates the locations of three typical NCOC constituent materials on the mid-wave IR glass map. The Abbe number ν of each of these glasses was computed using a modified formula for the Abbe number:

$$\nu = \frac{n_4 - 1}{n_3 - n_5} \tag{1}$$

where n_3, n_4, and n_5 are the refractive indices at 3, 4, and 5 μm, respectively. The refractive index and Abbe number of an NCOC made from the materials shown in Figure 2 can lie anywhere within the triangle defined by the end members. This allows for the image quality of an optical system to be better optimized by using NCOC lenses whose refractive index and Abbe number were chosen to maximize image quality.

Reflection, Scattering, and Diffraction from Surfaces, edited by Zu-Han Gu, Leonard M. Hanssen, Proc. of SPIE Vol. 7065, 70650B, (2008)
0277-786X/08/$18 · doi: 10.1117/12.792572

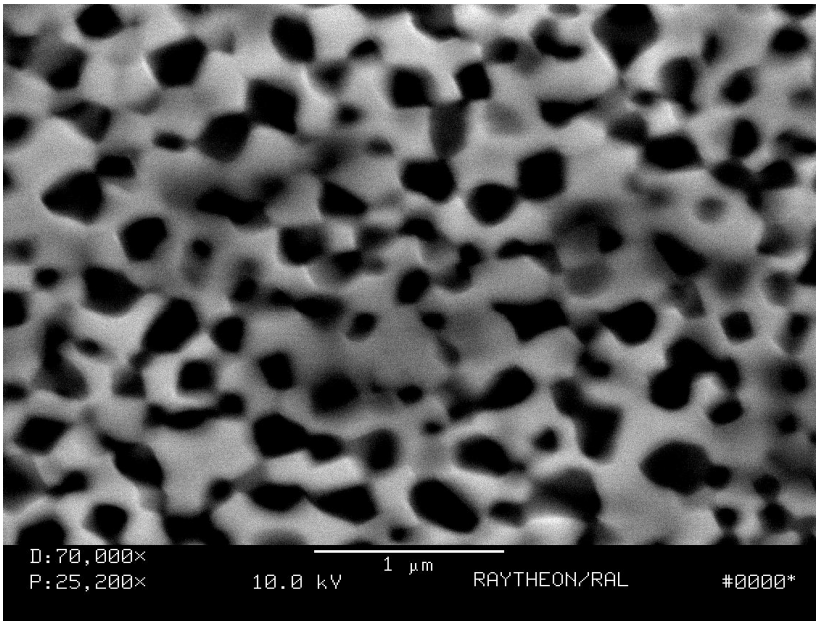

Figure 1. A scanning electron micrograph of a nanocomposite optical ceramic. The white areas are Y_2O_3 and the black are MgO.

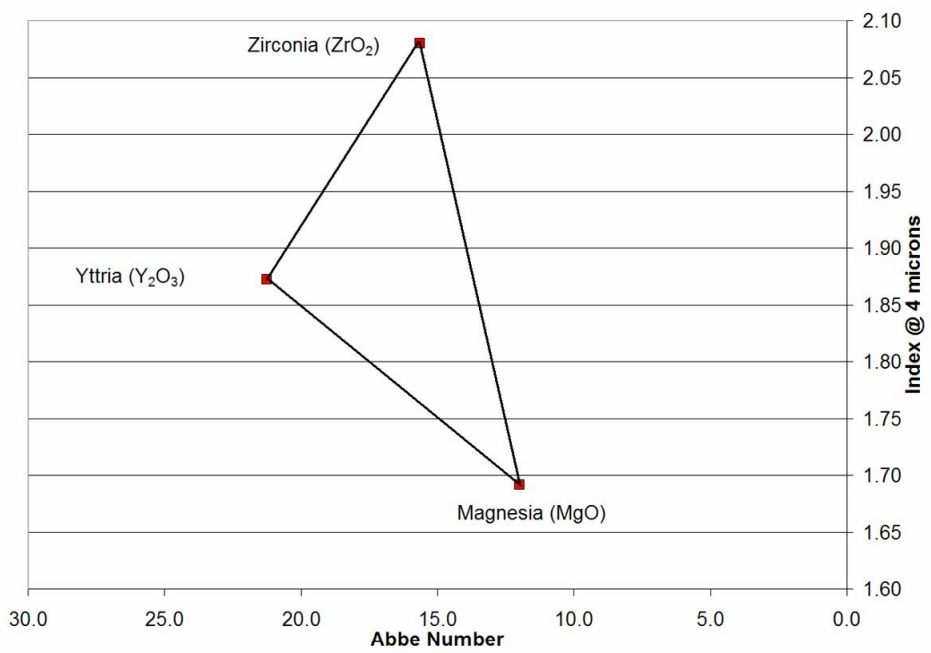

Figure 2. The mid-wave IR (3-5 µm) glass map with three typical NCOC constituent materials.

There are a tremendous number of variables to consider when developing an optical model of a composite material, such as the number and composition (i.e. complex refractive index) of constituent materials, their size relative to the

wavelength of incident light, their shape and arrangement inside the composite, to name a few. No single model can be used for all possible permutations of these variables, and since the model developed here primarily models NCOCs, this paper considers materials only with the following characteristics:

- The material is composed of particles that are roughly spherical in shape and of varying sizes (polydisperse).
- The particles are many times larger than their constituent molecules, and therefore they have the same refractive index as bulk samples
- The particles are arranged randomly, are fixed in place, and are densely packed, as shown in Figure 1.
- The particles are roughly the same size as the wavelength of incident light
- The particles can be lossy, as shown in Figure 3 for two typical constituents, Y_2O_3 and MgO.
- The particles and host medium are isotropic, non-magnetic, and do not exhibit non-linear optical effects

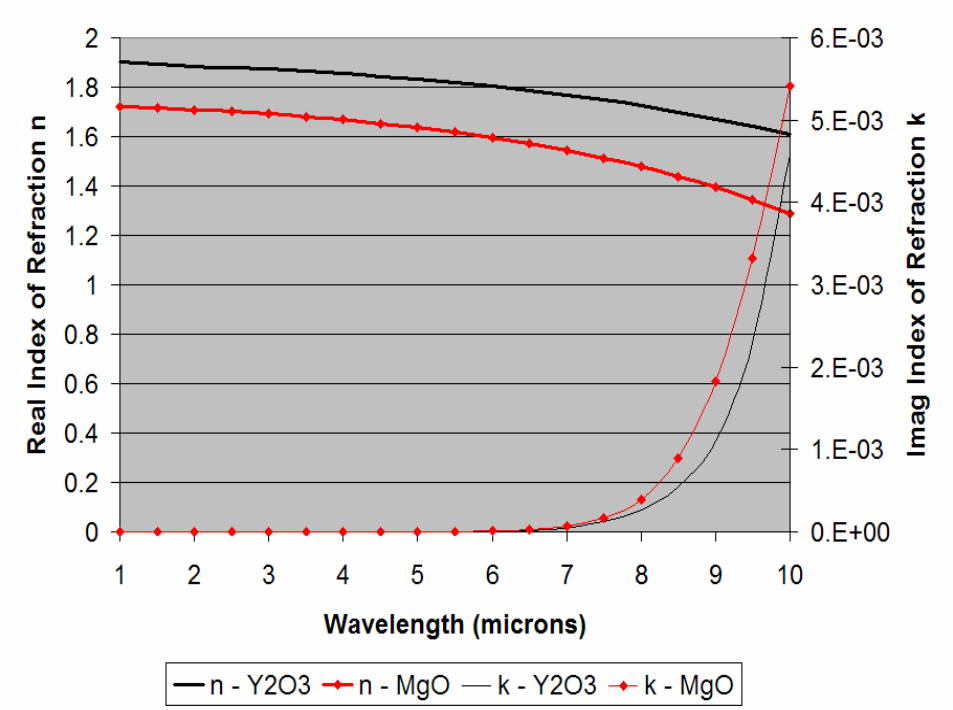

Figure 3. The real and imaginary parts of the refractive index for Y_2O_3 and MgO.

This paper is focused on establishing a particle scatter model that accurately predicts the optical performance (transmittance and BSDF) of NCOC materials with only a priori knowledge of the particles comprising the material, and does not discuss their fabrication. A predictive model based on solutions to Maxwell's equations is developed and implemented in a computer program. Predictions from this program are validated by comparing predicted to measured values. No specialized test equipment was developed to measure the optical performance of these materials; all measurements were performed using widely available test equipment. Comparisons of predicted and measured performance (transmittance and BSDF) are made for various NCOCs in the infrared (1-10 μm) and for Polycrystalline Alumina (PCA) in the visible and near-infrared (0.4-2.0 μm). PCA is a transmitting material used in high-temperature, corrosive environments such as high-pressure sodium lamps, and is evaluated in this paper because its structure is similar to that of NCOCs and it demonstrates a broader application of the developed model. Though NCOCs are

currently being developed for mid-wave infrared applications (3-5 μm), their performance is computed over a wider band to demonstrate broader applicability of the model.

2. METHODOLOGY

Model Development

The first step in the development of the scattering model is to choose an existing model as the basis. Many existing models can be applied to this problem, though none of them provide all of the desired modeling capabilities. In particular, few of the existing models explicitly compute BSDF, and therefore almost any model chosen as the basis will need to be extended to compute BSDF. Because NCOCs can consist of densely packed grains, as shown in Figure 1, a model that incorporates multiple scattering must be used. Multiple scattering models account for the coupling of electric fields between closely spaced particles, and are normally much more complex than single-scattering models (such as the Rayleigh [2] model), which do not account for such inter-particle effects. Because little data are available at this time which describes the internal geometric structure of NCOCs, the basis model must not require a detailed geometric description. The only available data consists of micrographs such as the one shown in Figure 1. Many of the more advanced multiple scattering computation methods (such as the T-matrix [3] and Discrete Dipole Approximation [4] methods) require detailed knowledge of the structure, and therefore may not be suitable for this modeling task.

A scatter model that fits these criteria was proposed in Durant et al. [5,6]. It can be used for densely packed particles (it will be shown that it works well even at 50% volume fraction), works for lossy media, and does not require exact knowledge of the structure of the material, though some statistical information about to the distribution of particles in the host media is necessary. In addition, this model reduces to a known result called the Foldy-Twersky approximation [7] if all of the scatterers are considered independent, which helps to confirm its validity. The end result of the model is an extinction coefficient for the material as a function of the complex refractive indices of its constituents and their size and statistical distribution. The extinction coefficient is computed by first approximating it assuming no interaction between the particles, using the scattering theory appropriate for the size and refractive index of the particles relative to the incident wavelength and host media, such as Rayleigh, Rayleigh-Gans, or Mie. This approximation is called the independent scattering approximation, and for the NCOCs and PCA considered in this paper the Rayleigh theory is applicable. The extinction coefficient is then refined by accounting for interactions between every pair of particles, then between every three particles, etc. until the solution converges. The final solution is called the dependent-scattering approximation. Since it is convenient to represent these higher-order interactions using schematic diagrams, this technique is often called *diagrammatic expansion*.

The materials considered in this paper consist of polydisperse particles, however, the basis model is derived only for mondisperse particles, and therefore it is necessary to extend the basis model. This derivation is lengthy and will not be reproduced here, but can be found in [8]. Essentially, the extinction coefficient and scattering matrix of materials consisting of polydisperse spheres is computed as a weighted average of those for mondisperse spheres. The basis model is also extended to compute BSDF by incorporating it in a Monte-Carlo raytracing simulation. This simulation is represented schematically in Figure 4. Rays are geometrically traced through a slab of the composite material, and the probability of a ray being scattered is given by the extinction coefficient of the material. The scattering matrix of the particle is then used to compute the direction of the scattered ray, and the raytrace continues until the ray is scattered again, absorbed, or refracts through the entrance or exit faces of the slab. Rays leaving the exit face are binned according to their scatter angle θ_s, and the flux in the bins is normalized to yield the BSDF of the slab.

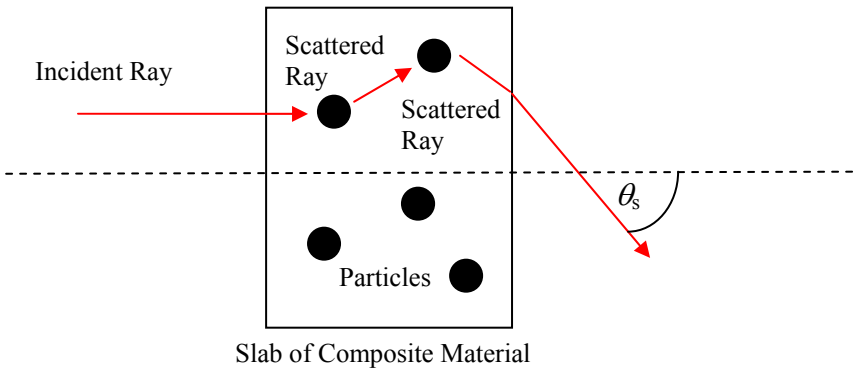

Figure 4. Schematic representation of Monte-Carlo raytrace used to compute the BSDF of a slab of composite material.

The sensitivity of the predicted transmittance and BSDF to changes in the input parameters is determined by making small changes (usually ±1%) to the inputs and computing the percent difference in the resulting transmittance and BSDF. The total uncertainty in the transmittance and BSDF predictions is computed by multiplying these sensitivities by the percent measurement uncertainties of the input parameters.

Derivation of Model Input Parameters

The input parameters for the model were determined using theoretical data and analysis of the measured samples. For NCOCs, the complex refractive indices of the particles and host media (MgO and Y_2O_3, respectively) were determined using the OPTIMATR computer program [9]. This program computes the indices using solid-state physics models of the materials. MgO was chosen as the particle material because the basis model works best when the particles have a low volume fraction, and the NCOC samples made for measurement have low volume fractions (<50%) of MgO. The size and distribution of the MgO particles were determined by analysis of SEMs of the samples [8]. The particles of MgO in the SEMs were rendered as circles, as shown in Figure 5, and the resulting distribution of circles was analyzed to extract the size and distribution of the corresponding distribution of spheres. The results of this analysis are the histograms shown in Figure 5.

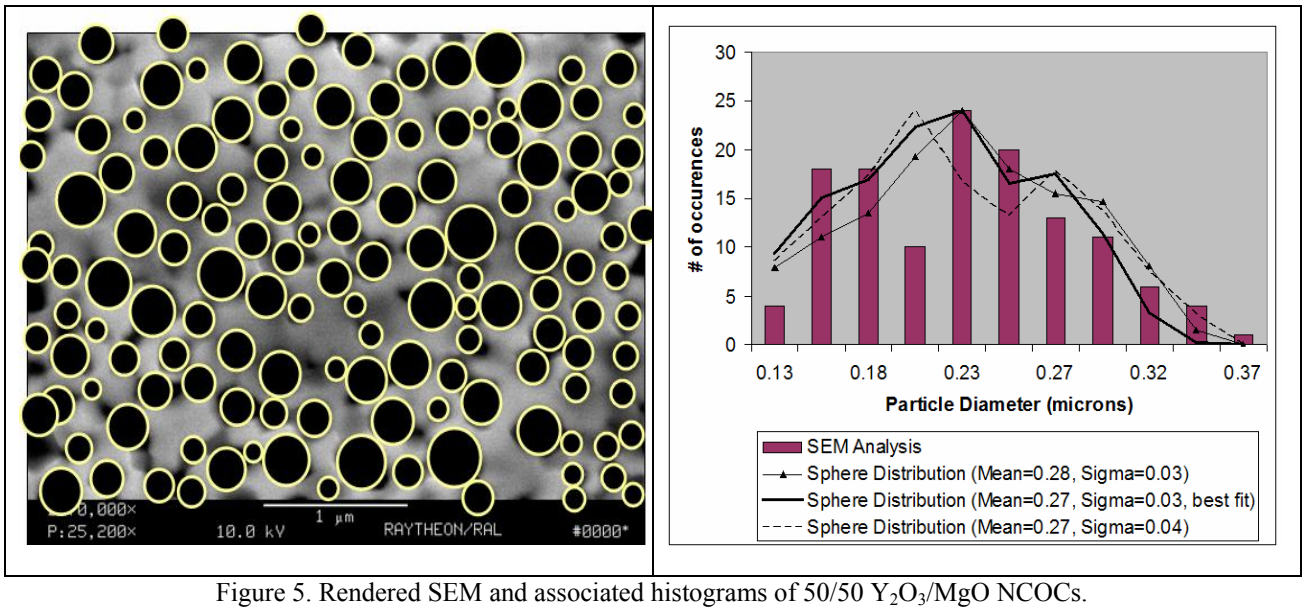

Figure 5. Rendered SEM and associated histograms of 50/50 Y_2O_3/MgO NCOCs.

The input parameters for PCA were the same as those determined in a previous analysis [10]. The material is modeled as a host medium with a refractive index of 1.76 containing a 50% volume of spheres (grains) of index 1.765 to 1.768 diameters of 0.5 μm. These input parameters neglect dispersion in the material.

The input parameter uncertainties used in this analysis are the minimum achievable for the given parameters and are not necessarily applicable to the transmittance and BSDF results shown below. For instance, the refractive index data currently used for the constituent materials was generated using the OPTIMATR software program, and it is not possible to know how accurate this data is since no refractive index measurements have been made of the constituent materials that are actually being used. Therefore, it is not possible at this time to assign a measurement uncertainty to this input parameter. However, it is known that refractive index can be measured to 0.1% using the "prism deviation" method, and therefore 0.1% is used as the measurement uncertainty in this paper. The measurement uncertainty for each input parameter is given in [8].

Sample Preparation and Measurement

The NCOC samples were fabricated as flat disks 1" in diameter and 0.75 mm thick. The entrance and exit faces of the disks were polished using conventional optical polishing techniques (rotary grind and ceramic lap). The RMS roughness of the entrance and exit faces is about 90 Å, and therefore we do not expect surface scatter to contribute significantly to the measured BSDF, given that the Total Integrated Scatter (TIS) of such a surface is given by

$$TIS = \left(\frac{\Delta n \pi \sigma}{\lambda} \right)^2 \tag{2}$$

where Δn is the refractive index difference between the substrate and the surrounding media (~0.7 for NCOCs), σ is the RMS surface roughness, and λ is the wavelength [11]. For a surface with 90 Å RMS roughness at 3.39 μm, the TIS is 0.018%, which is much less than the predicted loss due Fresnel reflections alone (~20%), and therefore can be neglected.

The transmittance measurements were performed using two instruments: a Cary 5000 UV-VIS-NIR spectrometer and a Bruker Equinox 55 FTIR spectrometer. The Cary can measure from 1 μm to 3.3 μm, and the Bruker from 3 to 10 μm, and therefore both must be used to cover the waveband of interest. The transmittance measurements from both instruments agree to within 3% for wavelengths in the overlap region (3 to 3.3 μm). Both devices use unpolarized light. The BSDF measurements were performed at 3.39 μm using a Schmitt Measurement Systems (SMS) CASI scatterometer. This instrument measures the angle-resolved BSDF using a detector mounted on the end of a goniometer that sweeps around the sample, as illustrated in Figure 6. The goniometer arm is 50 cm long, and the aperture of the detector varies from 1060 μm to 13860 μm to provide either high angular resolution near the specular peak (smaller aperture) or high signal-to-noise ratio away from the peak (large aperture). The polarization of the beam used to illuminated the sample can be oriented to be in the scatter measurement plane (p-polarized) or perpendicular to it (s-polarized).

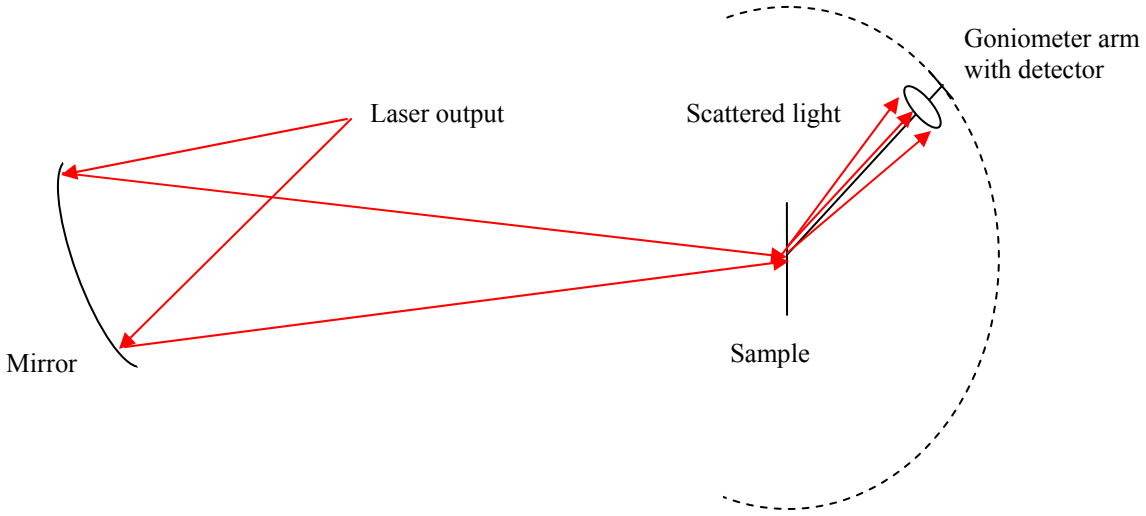

Figure 6. Optical layout of the CASI scatterometer

The PCA sample was fabricated with a thickness of 0.8 mm. The previous analysis [10] specifies only that the sample faces were "smooth", and do not indicate if (or how) they were polished and what the resulting RMS surface roughness was. It will be assumed that the entrance and exit faces of the slab were smooth enough that surface scattering can be neglected, as with NCOCs. The transmittance was measured using a spectrophotometer with a collection angle of 0.5°, which is a typical value. The make and model of the spectrophotometer is not given. BSDF measurements were not given in [10], and therefore no comparison with modeled BSDF will be made for PCA.

3. DATA AND RESULTS

Figure 7 shows the measured transmittance of the 0.75 mm thick NCOC samples for various volume fractions as well as the predicted transmittance using the independent and depdendent scattering models. Good correlation is obtained between dependent-scattering predictions and measurements for all three volume fractions. The plots show that both the (dependent) predictions and the measurements are fairly insensitive to the volume fraction of MgO. Comparison of the transmittance predicted using the independent and dependent scattering models shown in Figure 7 indicates the root cause of this phenomenon: as the particle volume fraction increases, the amount of scattering predicted by the independent scattering model increases and the transmittance drops, as expected. However, the effect of inter-particle interactions also increases with volume fraction, and in NCOCs these interactions (which are essentially interference effects) act to increase the transmittance, and the combination of these two effects leads to volume fraction insensitivity. At low volume fractions, the transmittance predicted using the independent and dependent models is almost identical due to the decrease in inter-particle effects, as shown in Figure 7 for the 90/10 Y_2O_3/MgO sample.

For NCOCs it is useful to divide the transmission spectrum into the two regions: the first region is called the transition region, and occurs from 1-3 μm and from 5-10 μm. In this region, the transmission changes rapidly as a function of wavelength due to either scattering by the particles or absorption by the particles and the host media. This represents the transmittance cut-on and cut-off regions of the material and therefore the uncertainty in transmittance is highest in this region. The second region is called the plateau region, and occurs from 3-5 μm. This region is characterized by slowly changing transmittance versus wavelength, and therefore the uncertainty in transmittance is lower in this region. NCOCs are being developed for sensors that operate in the plateau region, and therefore transmittance predictions made for this region are of greater importance than those made for the transition region.

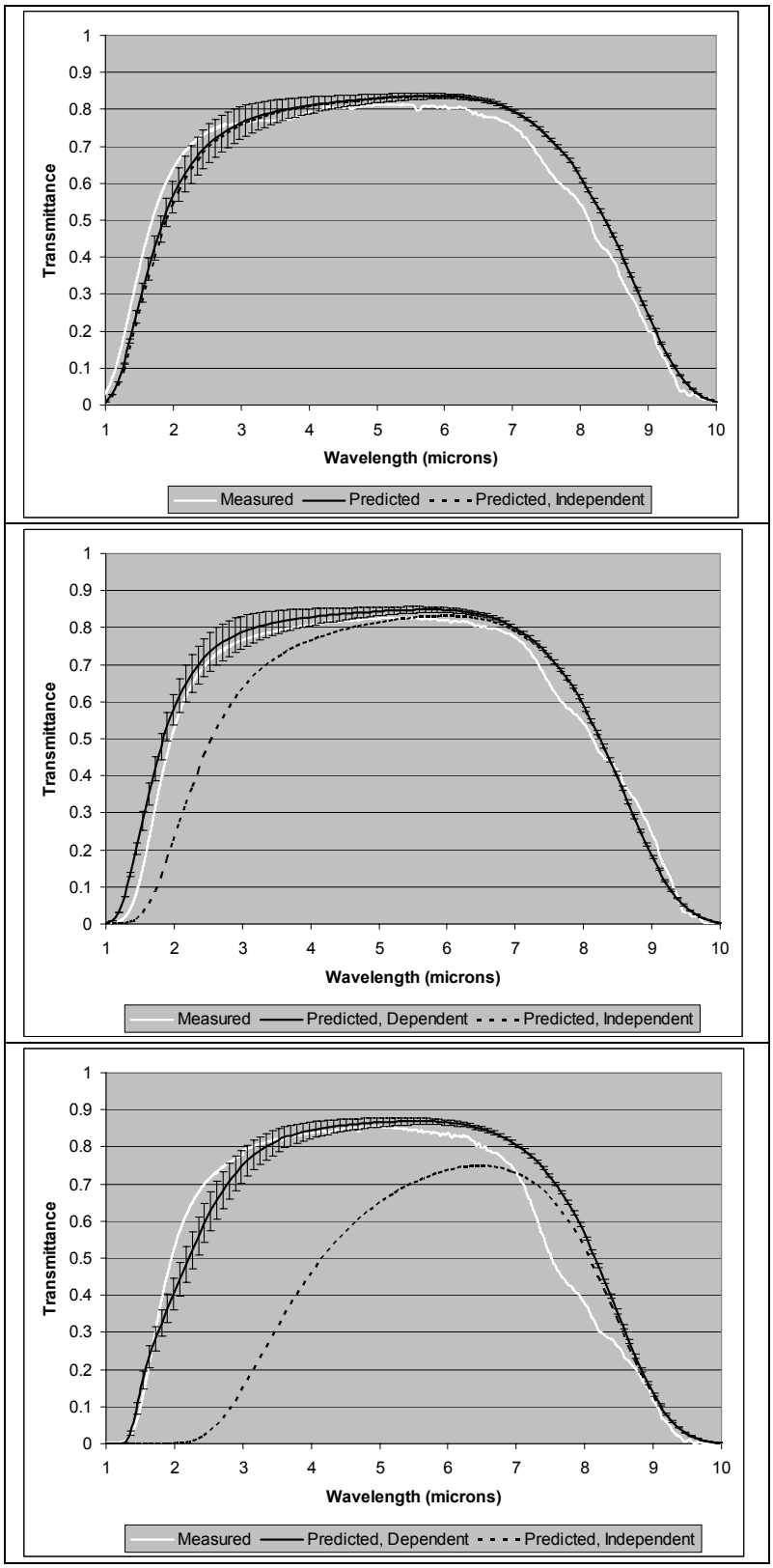

Figure 7. Measured and predicted transmittance for a 0.75 mm thick 90/10 (top), 70/30 (middle), and 50/50 (bottom) Y_2O_3/MgO NCOC. Error bars are shown for the predicted dependent transmittance.

The predicted transmittance for all three NCOCs analyzed matches the measurements to within the predicted uncertainty for all wavelengths in the plateau region (3-5 μm) except for a small wavelength range near 5 μm. As discussed earlier, the accuracy of predicted transmittance is more important in the plateau region than in the transition region because this is the intended region of use. Therefore, Figure 7 demonstrates that the model developed here can be used to predict transmittance in the plateau region to within the uncertainty given by the input parameter uncertainty. In the transition region, the predicted transmittance for all three NCOCs analyzed deviates from the measurements by more than the predicted uncertainty for a significant fraction of the transition region. This discrepancy is explained by the fact that the uncertainty values shown in Figure 7 are achievable only if the input parameters are known to within the uncertainties given in [8]. For this analysis, the input parameters may have higher uncertainties, and therefore uncertainty in transmittance may be higher.

Comparison of the predicted and measured BSDF is shown in Figure 8. The predictions were made using the dependent-scattering model. The predicted BSDF roughly agrees with the measured, and both vary in the same way with input polarization. The polarization dependence is due to the fact that the scatter plane contains more energy when the incident beam is s-polarized than when it's p-polarized, as predicted by the Rayleigh scattering theory [12]. SEM analysis of the samples indicated the presence of a low volume fraction of metal particles, and the lower plot in Figure 8 shows that the predicted BSDF agrees with the measured BSDF better if these particles are included in the predictions. This suggests that angle-resolved BSDF measurements can be used as a diagnostic tool to study the composition of composite materials. Adding the metal spheres had very little effect (<5%) on the predicted transmittance, so transmittance measurements alone would not have been sufficient to identify the presence of contaminants. As with the transmittance predictions, the BSDF predictions agree with the measurements to within the uncertainty provided reasonable values are assumed for the uncertainty of the input parameters.

The measured and predicted transmittance for PCA is shown in Figure 9. Data for the measured curve was obtained from the paper using a digitizing program. The curves match quite closely, though the model underpredicts the extinction at shorter wavelengths and overpredicts it at longer wavelengths. At most wavelengths, the predicted transmittance matches the measured to within the model uncertainty for PCA determined earlier. However, the two disagree at the shorter wavelengths. As with NCOCs, this can be explained by the fact that the uncertainties determined earlier are best-case uncertainties, and the uncertainties in the input parameters used in this prediction may have been higher. The uncertainty analysis for PCA suggests that uncertainty in the real refractive index of the particle is the major contributor to uncertainty in the transmittance prediction, and that an uncertainty of 0.2% in refractive index (a reasonable value) is sufficient to explain the discrepancy between the prediction and the measurement.

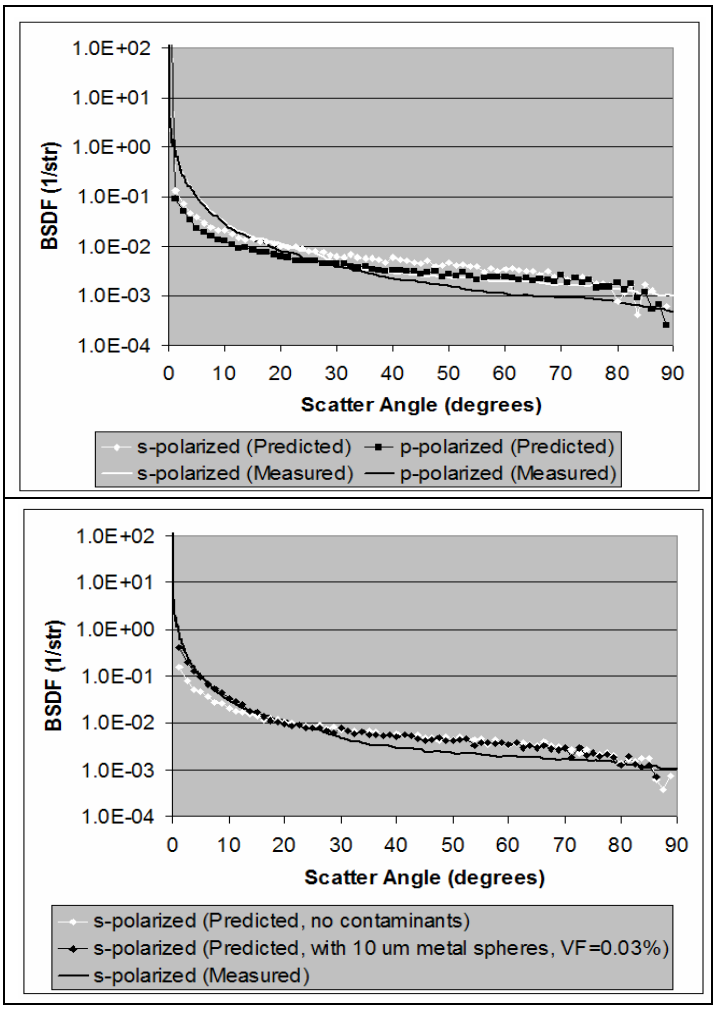

Figure 8. Measured and predicted BSDF of a 0.75 mm thick Y_2O_3/MgO NCOC at 3.39 μm with no contaminants (top) and with a 0.03% volume fraction of 10 μm diameter metal spheres (bottom).

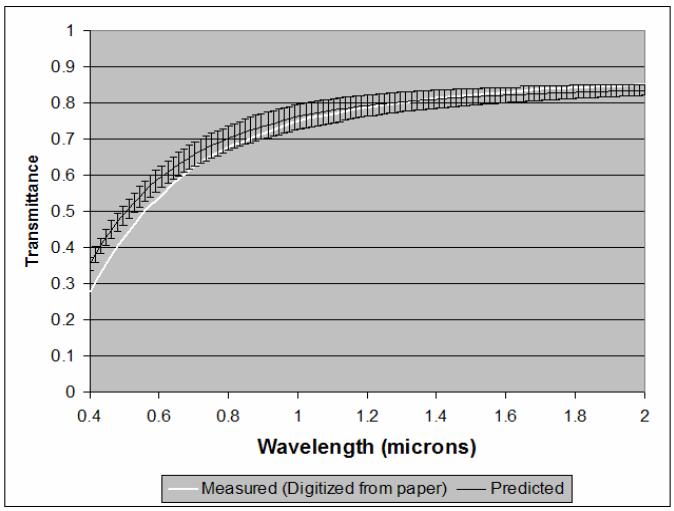

Figure 9. Measured and predicted transmittance for a 0.8 mm thick PCA sample. Error bars are shown for the predicted transmittance.

4. CONCLUSIONS

Measured and predicted transmittance and BSDF curves are compared for NCOCs and for PCA. The major features in the predicted curves, such as transmittance cut-on and cut-off wavelengths and the volume fraction insensitivity seen in NCOCs, closely match those in measured curves. Because the transmittance of NCOC optical elements is insensitive to the volume fractions of their constituent materials, their compositions can be varied to maximize the image quality in an optical system without sacrificing transmittance. For NCOCs in the plateau region (3-5 μm), the predicted transmittance matches the measured to within the predicted uncertainty for all NCOCs measured. This demonstrates that the model developed here can be used to predict transmittance in the plateau region to within the transmittance uncertainty given by the uncertainty in the input parameters. In the transition region (1-3 μm, 5-10 μm), the predicted transmittance for two of the samples (70/30 and 90/10) match the measurements to within the transmittance uncertainty. The predicted transmittance for the third NCOC sample (50/50) and for the PCA sample deviate from the measured by more than the predicted uncertainty, which can be explained by the fact that the uncertainties determined in the previous chapter are best-case and may not apply to the input parameters used in the predictions shown here. Reasonable assumptions about the true uncertainty of the input parameters used in these predictions can explain the discrepancies between predicted and measured transmittance. Comparison of the measured and predicted BSDF for an NCOC sample indicates that the model correctly predicts the variation in BSDF with input polarization and confirms the presence of a small volume fraction of large metal contaminants. This suggests that BSDF measurements can be used to test the composition of composite materials.

The implementation of the model derived in this paper is sufficient for modeling NCOCs and PCA. However, there are many ways it can be made more accurate. The complex refractive index data for Y_2O_3 and MgO were obtained from the OPTIMATR program, however, a more accurate means of obtaining this data would be to measure the refractive indices of actual sample materials used in NCOC fabrication, using prism-deviation or other refractive index measurement techniques. The particle size distributions for NCOCs were derived from SEMs which contained, at most, 145 particles. Making SEMs that contain more particles would obviously increase the fidelity of the model. The particles in the SEMs analyzed for this paper were sized and counted by hand, however, if larger SEMs were available, it may be necessary to use or develop an image-processing program in order to obtain the particle-size distribution data in a reasonable amount of time. Even better than taking SEMs of the materials would be to analyze them using x-ray tomography, which would give the 3-D distribution of the particles. Doing so would almost certainly require the use or development of computer software to perform these calculations on large sets of data. Further testing of the model by comparing its predictions to measurements from composite materials whose constituents are different than those considered here is necessary to prove the model's broader application.

ACKNOWLEDGEMENTS

I would also like to acknowledge all those affiliated with the DARPA Nanocomposite Oxides contract, including John McCloy, Rick Gentilman, Larry Kabacoff, Sharon Beermann-Curtin, Marie Sandrock, Dan Harris, Scott Nordahl, Brian Zelinksi, and Howard Poisl. Their support has made this research possible.

REFERENCES

1. Harris, D. C., *Materials for Infrared Windows and Domes*, SPIE Optical Engineering Press, 119-120, (1999)
2. Rayleigh, Lord, "On the light from the sky, its polarization and colour", Philos. Mag. 41, 107-120, 274-279 (1871). Repreinted in *Scientific Papers by Lord Rayleigh,* Vol. I, No. 8, Dover, New York, 1869-1881 (1964)
3. Mishchenko, M. I., Travis, L. D., and Mackowski, D. W., "T-Matrix computations of light scattering by non-spherical particles: a review", J. Quant. Spectroc. Radiat. Transfer 55(5), 535-575 (1996)
4. Draine, B. T. and Flatau, P. J., "Discrete dipole approximation for scattering calculations", J. Opt. Soc. Am. A 11(4), 1491 (1994)

5. Durant, S., Calvo-Perez, O., Vukadinovic, N., and Greffet, J-J., "Light scattering by a random distribution of particles embedded in absorbing media: diagrammatic expansion of the extinction coefficient", J. Opt. Soc. Am. 24(9), 2953-2962 (2007)
6. Durant, S., Calvo-Perez, O., Vukadinovic, N., Greffet, J-J., "Light scattering by a random distribution of particles embedded in absorbing media: full-wave Monte Carlo solutions of the extinction coefficient", J. Opt. Soc. Am. A 24(9), 2953-2962 (2007)
7. Twersky, V., "On propagation in random media of discrete scatterers", Proc. Am. Math Soc. 16, 84-116 (1964)
8. Fest, E. C., "Modeling scatter in composite media", Ph.D. dissertation thesis, The University of Arizona (2008)
9. OPTIMATR computer program, Johns Hopkins University Applied Physics Lab (1991 version)
10. Apetz, R. and van Bruggen, M. P. B., "Transparent Alumina: A Light-Scattering Model", J. Am . Ceram. Soc. 86(3), 480-86 (2003)
11. ASAP Software User's Manual, Breault Research organization, "Scatter modeling" chapter.
12. Bohren, C. F. and Huffman, D. R., *Absorption and Scattering of Light by Small Particles*, Wiley, 130-136 (1983)